Journal of Materials Chemistry

Cite this: *J. Mater. Chem.*, 2012, **22**, 17724

www.rsc.org/materials

PAPER

A new benzo[1,2-*b*:4,5-*b*′]difuran-based copolymer for efficient polymer solar cells†

Xuewen Chen,‡[a] Bo Liu,‡[ab] Yingping Zou,*[ab] Lu Xiao,[a] Xiuping Guo,[a] Yuehui He[b] and Yongfang Li[c]

Received 6th May 2012, Accepted 9th June 2012
DOI: 10.1039/c2jm32843g

A new donor–acceptor type copolymer, namely poly{4,8-bis(2-ethylhexyloxy)benzo[1,2-*b*:3,4-*b*′]difuran-*alt*-6-octylnaphtho[2,3-*c*]thiophene-4,9-dione} (PBDFNTDO) was synthesized by a Stille coupling reaction and characterized by ^{1}H NMR, GPC, TGA, UV-Vis absorption spectroscopy and cyclic voltammetry. PBDFNTDO is readily soluble in common organic solvents with a number-average molecular weight (M_n) of 10.7 kDa mol^{-1} and a polydispersity index of 1.71. TGA analysis shows the copolymer exhibits good thermal stability with 5% weight loss at a temperature of 341 °C. PBDFNTDO possesses a broad absorption band at 300–750 nm with an optical bandgap of 1.65 eV. Cyclic voltammetry gives HOMO and LUMO energy levels of −5.33 eV and −3.40 eV, respectively. The hole mobility of PBDFNTDO:$PC_{71}BM$ (1 : 1.5, w/w) reaches up to 5.0×10^{-3} cm^2 V^{-1} s^{-1} by the space-charge-limited current (SCLC) method. A polymer solar cell with the configuration of ITO/PEDOT:PSS/PBDFNTDO:$PC_{71}BM$ (1 : 1.5, w/w)/Ca/Al demonstrates a promising power conversion efficiency of 4.71% under the illumination of AM 1.5 G, 100 mW cm^{-2}.

1. Introduction

In the past two decades, conjugated polymers have attracted much interest in polymer solar cells (PSCs),[1] field-effect transistors (FETs)[2] and light-emitting diodes (LEDs),[3] because of their advantages of being light-weight, flexible and low-cost.[4–8] PSCs are composed of a photoactive blend layer of a conjugated polymer donor and a soluble fullerene derivative acceptor sandwiched between an indium-tin oxide (ITO) positive electrode and a low work function metal negative electrode.[9–11] The photoactive layer of PSCs consists of a network formed by an electron-donor (D) blended with an electron-acceptor (A).[12] Recently, a D–A type conjugated polymer showed excellent properties and this kind of polymer plays an important role in the PSCs field.[13]

Benzo[1,2-*b*:4,5-*b*′]dithiophene (BDT) as electron-donor unit has attracted broad attention because BDT-based copolymers possessed high efficiencies of up to 8%.[14] Many BDT based conjugated polymers with different electron acceptor units, such as 2,1,3-benzothiadiazole (BT),[15] thieno[3,4-*c*]pyrrole-4,6-dione (TPD),[16] thieno[3,4-*b*]thiophene (TT),[17] pyrrolo[3,4-*c*]-pyrrole-1,4-dione (DPP),[18] *etc.* exhibited promising photovoltaic properties. For example, Hou *et al.* reported an alternating copolymer of BDT and TT, namely PBDTTT-CF, and obtained a high power conversion efficiency (PCE) of up to 7.7%.[19]

Benzo[1,2-*b*:4,5-*b*′]difuran (BDF) has a similar structure compared with the BDT unit, although the oxygen atom has a smaller diameter and higher electronegativity than a sulfur atom. BDF-based copolymers may form a good planar and stacking structure when combined with a suitable acceptor moiety, and then better absorbance and higher mobility are expected, which can lead to high photovoltaic properties.

The naphtho[2,3-*c*]thiophene-4,9-dione (NTDO) unit possesses a relatively simple, planar structure and has strong electron withdrawing ability resulting in lower HOMO and LUMO energy levels of the D–A copolymers.[20] Usually a lower HOMO level is beneficial to get higher open circuit voltages (V_{oc}) of the PSCs.

Taking all of these results into account, the development of new low band-gap BDF based copolymers with NTDO as the electron accepting unit should therefore lead to some interesting features for photovoltaic applications. In this work, we synthesized a new D–A copolymer, namely poly{4,8-bis(2-ethylhexyloxy)benzo[1,2-*b*:3,4-*b*′]difuran-*alt*-6-octylnaphtho[2,3-*c*]thiophene-4,9-dione} PBDFNTDO and our recently synthesized similar polymer PBDTNTDO-C3 is introduced for comparison (see Scheme 1). However, when preparing our manuscript, Huo *et al.* reported an interesting BDF based copolymer (PBDFDTBT) with a high PCE of up to 5% after thermal

[a]*College of Chemistry and Chemical Engineering, Central South University, Changsha 410083, China. E-mail: yingpingzou@csu.edu.cn*
[b]*State key Laboratory for Powder Metallurgy, Central South University, Changsha 410083, China*
[c]*Beijing National Laboratory for Molecular Sciences, Institute of Chemistry, Chinese Academy of Sciences, Beijing 100190, China*

† Electronic supplementary information (ESI) available: Fabrications of OFET devices and Fig. S1 giving the output characteristics and transfer characteristics of PBDFNTDO thin films, Fig. S2 giving the *J–V* curves of the devices with some modifications and Table S1 giving the corresponding photovoltaic data. See DOI: 10.1039/c2jm32843g

‡ X. Chen and B. Liu contributed equally to this work.

annealing,[21] which is much higher than that of its most similar BDT based polymer-Z3 with a PCE of 1.95%:[22] this first publication about BDF based polymers further confirmed our prediction. Herein, our new polymer is well characterized and the properties are investigated in detail. PBDFNTDO is soluble in common organic solvents, such as chloroform, toluene and *o*-dichlorobenzene, *etc.* with excellent film forming properties. PBDFNTDO film shows a broad absorption edge at 750 nm with an optical band-gap (E_g) of 1.65 eV. The PSC devices based on PBDFNTDO as the donor and $PC_{71}BM$ as the acceptor indicate a high PCE of 4.71%, with a short circuit current (J_{sc}) of 9.14 mA cm^{-2}, an open circuit voltage (V_{oc}) of 0.87 V and a fill factor (FF) of 0.59 under the illumination of AM 1.5 G, 100 mW cm^{-2}. These results indicate that BDF probably would be a promising electron donor building block for efficient PSCs.

2. Experimental

2.1 Materials

Furan-3-carboxylic acid, *n*-BuLi, $Pd(PPh_3)_4$ and $Sn(CH_3)_3Cl$ were obtained from Acros Organics, and they were used as received. Tetrahydrofuran (THF) was dried over Na/benzophenone ketyl and freshly distilled prior to use. Other reagents and solvents were purchased commercially as analytical-grade quality and used without further purification. 1,3-Dibromo-6-octylnaphtho[2,3-*c*]thiophene-4,9-dione has been synthesized according to our group's recently submitted manuscript.[23] All the other compounds were synthesized following the procedures described here.

2.2 Characterization

^1H NMR and ^{13}C NMR spectra were recorded using a Bruker DMX-400 spectrometer, chemical shifts were reported as δ values (ppm) relative to an internal tetramethylsilane (TMS) standard. Number-average (M_n) and weight-average (M_w) molecular weights were measured by GPC, using polystyrene as a standard. TGA was performed on a PE TGA-7 at a heating rate of 20 K min^{-1} under a nitrogen atmosphere. UV-vis absorption spectra were taken using a Hitachi U-3010 UV-Vis spectrophotometer. For solid state measurements, a polymer solution in chloroform was cast onto quartz plates. Optical bandgaps were calculated from the onset of the absorption band. Cyclic voltammograms (CV) were recorded on a Zahner IM6e Electrochemical Workstation using a platinum disk coated with the polymer film, Pt wire and a Ag/Ag^+ (0.1 M $AgNO_3$ in acetonitrile) reference electrode in an anhydrous and argon-saturated solution, as working electrode, counter electrode and reference electrode, respectively, in a 0.1 mol L^{-1} tetrabutylammonium hexafluorophosphate (Bu_4NPF_6) acetonitrile solution at a scan rate of 50 mV s^{-1}. The HOMO and LUMO energy levels were determined from the oxidation and reduction onsets from CV spectra. Electrochemical onsets were determined at the position where the current started to differ from the baseline. X-ray diffraction (XRD) measurements of the polymer thin films were carried out with a 2 kW Rigaku X-ray diffraction system. XRD patterns were obtained using Bragg-Brentano Geometry (θ–2θ) with Cu Kα radiation as an X-ray source in the reflection mode at 45 kV and 300 mA. AFM images were obtained using a Veeco's Dimension V atomic force microscopic (AFM) in the tapping mode.

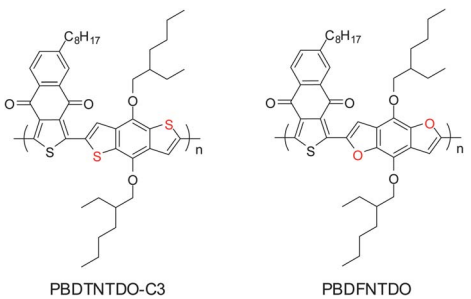

Scheme 1 Chemical structures of PBDTNTDO-C3 and PBDFNTDO.

2.3 Fabrication and characterization of polymer solar cells

The PSCs were fabricated in the configuration of the traditional sandwich structure with an indium-tin oxide (ITO) glass positive electrode and a metal negative electrode. Patterned ITO glass with a sheet resistance of 10 $\Omega\ \square^{-1}$ was purchased from CSG HOLDING Co. LTD. (China). The ITO glass was cleaned by sequential ultrasonic treatments in detergent, deionized water, acetone and isopropanol, and then treated in an ultraviolet-ozone chamber (Ultraviolet Ozone Cleaner, Jelight Company, USA) for 20 min. The PEDOT:PSS (poly(3,4-ethylene dioxythiophene):poly(styrene sulfonate)) (Baytron P 4083, Germany) was filtered through a 0.45 μm filter and spin coated at 2000 rpm for 60 s on the ITO electrode. Subsequently, the PEDOT:PSS film was baked at 150 °C for 15 min in air to give a thin film with a thickness of 40 nm. A blend of the polymer and $PC_{71}BM$ (1 : 1 w/w, 10 mg mL^{-1} of polymer) was dissolved in *o*-dichlorobenzene (ODCB), and spin-cast at 3000 rpm for 45 s onto the PEDOT:PSS layer. The substrates were then dried at 70 °C for 15 min. The thickness of the photoactive layer is in the range of 70–80 nm measured by an Ambios Technology XP-2 profilometer. A bilayer cathode consisting of Ca (~20 nm) capped with Al (~60 nm) was thermally evaporated under a shadow mask with a base pressure of *ca.* 10^{-5} Pa. The active area of the PSCs is 4 mm^2. Device characterization was carried out under AM 1.5 G irradiation with the intensity of 100 mW cm^{-2} (Oriel 67005, 500 W) calibrated by a standard silicon cell. *J*–*V* curves were recorded with a Keithley 236 digital source meter.

2.4 Synthesis of the monomer and polymer

Furan-3-carbonyl chloride (1). A mixture of furan-3-carboxylic acid (25.1 g, 0.224 mol) and thionyl chloride (65.3 mL, 0.90 mol) was refluxed for 4 h. To the reaction mixture was added dry benzene (60 mL), and the solution was distilled to remove any excess of thionyl chloride and benzene, the brown liquid was used in the next step without further purification.

***N*,*N*-Diethylfuran-3-carboxamide (2).** Compound **1** was added dropwise to a solution of diethylamine (92.6 mL) in dry CH_2Cl_2 (100 mL) at 0 °C, the solution was then stirred at room temperature and poured into iced water. The reaction solution was extracted three times with CH_2Cl_2. The combined organic

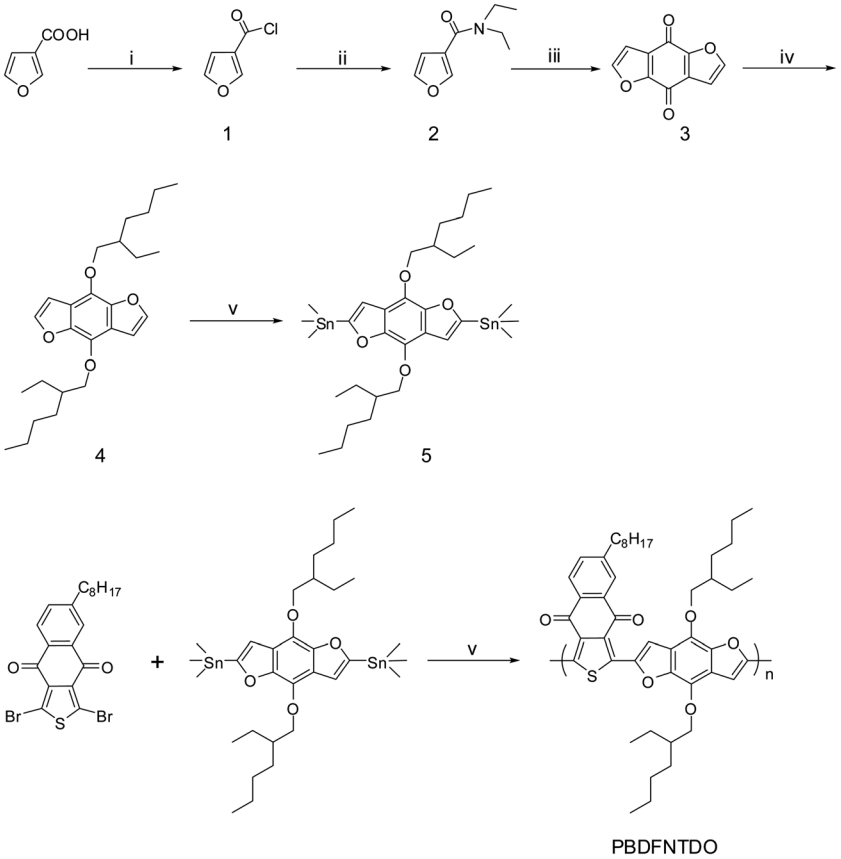

Scheme 2 Synthesis of the comonomer and PBDFNTDO: (i) $SOCl_2$, reflux, 4 h; (ii) $N(CH_3CH_2)_2$, CH_2Cl_2, rt, 1 h; (iii) *n*-BuLi, THF, 0 °C; then rt, overnight; (iv) 2-ethylhexyl bromide, NaOH, Zn, H_2O, $N(C_4H_9)_4Br$, reflux, overnight; (v) *n*-BuLi, THF, −78 °C; then $Sn(CH_3)_3Cl$, rt, overnight; (vi) $Pd(PPh_3)_4$, toluene, 110 °C, 48 h.

extractions were washed with dilute hydrochloric acid and water successively, dried over $MgSO_4$ and then evaporated. The crude product was purified by chromatography on silica gel (elution with ethyl acetate/hexane = 2/1). Compound **2** was isolated (30.3 g, 81%) as a colorless oil: GC-MS: m/z = 167. ^{1}H NMR (400 MHz, $CDCl_3$, ppm): 7.72 (d, 1H), 7.44 (d, 1H), 6.65 (d, 1H), 3.48 (q, 4H), 1.20 (t, 6H).

Benzo[1,2-*b*:4,5-*b*′]difuran-4,8-dione (3). Compound **2** (8.35 g, 0.05 mol) was put into a well-dried flask with 50 mL THF under an inert atmosphere. The solution was cooled down in an ice-water bath, and 21 mL *n*-butyllithium (0.05 mol, 2.4 mol L^{-1}) were added to the flask dropwise over 30 min. Then the reaction mixture was stirred at ambient temperature for 14 h. The reaction mixture was poured into 500 g ice-water and stirred overnight. The mixture was filtered, the yellow precipitate was washed by water, methanol, and hexane successively. Compound **3** was obtained as a yellow powder (1.6 g, 34%). GC-MS: m/z = 188. ^{1}H NMR (400 MHz, $CDCl_3$, ppm): 7.72 (s, 2H), 6.94 (s, 2H).

4,8-Bis(2-ethylhexyloxy)benzo[1,2-*b*:3,4-*b*′]difuran (4). Compound **3** (4.4 g, 20 mmol), zinc powder (1.88 g, 10 mmol) and 33 mL water were put into a 100 mL flask; then 6 g of NaOH were added to the mixture. The mixture was stirred well and heated to reflux for 1 h. Then, 1-bromoethylhexane (5.8 g, 30 mmol) and a catalytic amount of tetrabutylammonium bromide were added to the flask. Then, the reaction mixture was refluxed overnight. The reaction mixture was poured into cold water and extracted by CH_2Cl_2. The organic layer was dried over anhydrous $MgSO_4$. After removing the solvent, the crude product was purified by column chromatography on silica gel using petroleum ether as eluent. Compound **4** was obtained as a pale yellow oil (2.2 g, yield: 53%). GC-MS: m/z = 414. ^{1}H NMR (400 MHz, $CDCl_3$, ppm): 7.87 (m, 2H), 7.37 (m, 2H), 4.72 (t, 2H), 2.12 (m, 2H), 1.34–1.22 (m, 10H), 0.86 (t, 3H). ^{13}C NMR ($CDCl_3$, 100 MHz), δ (ppm): δ 144.09, 142.47, 131.35, 119.42, 104.65, 75.52, 40.24, 30.40, 29.15, 23.68, 23.18, 14.15, 11.19.

2,6-Bis(trimethyltin)-4,8-bis(2-ethylhexyloxy)benzo[1,2-*b*:3,4-*b*′]difuran (5). Compound **4** (0.83 g, 2 mmol) and 30 mL dry THF were added to a flask under an inert atmosphere. The solution was cooled down to −78 °C and 2.9 mL *n*-butyllithium (7.0 mmol, 2.4 mol L^{-1}) were added dropwise. After being stirred at −78 °C for 1 h, 8 mL trimethyltin chloride (8.0 mmol, 1 mol L^{-1}) were added in one portion, the cooling bath was removed, and the reaction mixture was stirred at ambient temperature overnight. Finally it was poured into 100 mL ice-water and extracted by CH_2Cl_2. The organic layer was washed by water twice, then dried over anhydrous $MgSO_4$, and evaporated to give a yellow oil which was slowly crystallized. The residue was

recrystallized from isopropanol to yield the target monomer as colorless needles (0.74 g, 50%). GC-MS: m/z = 740. ^{1}H NMR (400 MHz, $CDCl_3$, ppm): 7.04 (s, 2H), 4.32 (d, 4H), 1.75 (m, 2H), 1.55–1.34 (m, 16H), 0.97 (m, 12H), 0.41 (s, 18H). ^{13}C NMR (100 MHz, $CDCl_3$, ppm): δ 164.15, 146.21, 129.95, 120.01, 115.40, 75.34, 40.25, 30.63, 29.20, 23.93, 23.27, 14.28, 11.26, −9.12.

Poly{4,8-bis(2-ethylhexyloxy)benzo[1,2-*b*:3,4-*b*′]difuran-*alt*-6-hexylnaphtho[2,3-*c*]thiophene-4,9-dione} (PBDFNTDO). Compound **5** (0.148 g, 0.2 mmol), 1,3-dibromo-6-octylnaphtho[2,3-*c*]thiophene-4,9-dione (0.097 g, 0.2 mmol) and 10 mL dry toluene were put into a two-necked flask. The solution was flushed with N_2 for 10 min, then $Pd(PPh_3)_4$ (12 mg) was added to the flask. The solution was flushed with N_2 again for 25 min. The oil bath was heated to 110 °C carefully, and the reaction mixture was stirred for 48 h at this temperature under N_2 atmosphere. Then the reaction mixture was cooled to room temperature and the polymer was precipitated by the addition of 100 mL methanol and filtered through a Soxhlet thimble, which was then subjected to Soxhlet extraction with methanol, hexane and chloroform. The polymer was recovered as a solid from the chloroform fraction by rotary evaporation. The blue solid was dried under vacuum at 40 °C overnight (64 mg, yield: 26%). ^{1}H NMR (400 MHz, $CDCl_3$): 8.31 (d, 2H), 8.22 (s, 1H), 7.66 (d, 1H), 7.08 (s, 2H), 4.34 (d, 4H), 1.78–1.04 (m, 42H), 0.81–0.96 (m, 15H). Anal. calcd for $(C_{58}H_{76}N_2O_4S_2)_n$ (%): C, 75.16; H, 8.15; O, 12.51; S, 4.18. Found (%): C, 75.48; H, 8.23; O, 12.19; S, 4.22%.

3. Results and discussion

3.1 Synthesis and characterization of PBDFNTDO

The synthetic routes to the monomer and PBDFNTDO are illustrated in Scheme 2. The polymer was synthesized with 2,6-bis(trimethyltin)-4,8-bis(2-ethylhexyloxy)benzo[1,2-*b*:3,4-*b*′]difuran (**5**) and 1,3-dibromo-6-octylnaphtho[2,3-*c*]thiophene-4,9-dione using a typical Stille coupling polymerization reaction. PBDFNTDO was purified by continuous extraction with methanol, hexane and chloroform, the chloroform fractions were recovered. Gel permeation chromatography (GPC) results (using polystyrene as the standard and THF as eluent) have shown that the polymer has a number-average molecular weight (M_n) of 10.7 kDa mol^{-1} with a polydispersity index of 1.71. The copolymer is readily soluble in common organic solvents such as chlorobenzene, dichlorobenzene and tetrahydrofuran, *etc.*

3.2 Thermal stability

Thermal stability of the polymer is important for device fabrication. Fig. 1 displays the TGA thermogram of PBDFNTDO. TGA analysis reveals that, under the protection of an inert atmosphere, the onset point of the weight loss (5%) of PBDFNTDO is *ca.* 341 °C. High thermal stability of the resulting copolymer prevents the deformation of the copolymer morphology and the degradation of the polymeric active layer under applied electric fields.

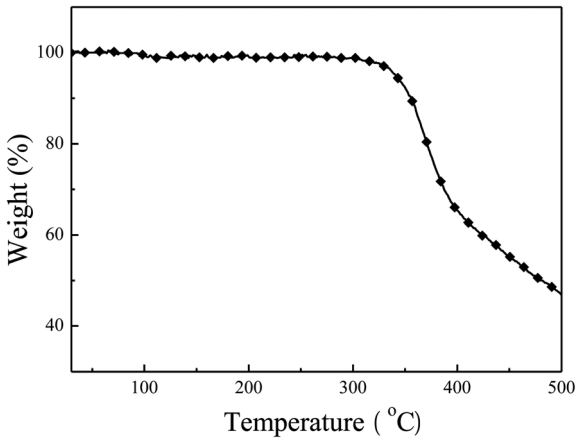

Fig. 1 TGA thermogram of PBDFNTDO with a heating rate of 10 K min^{-1}.

3.3 Optical properties

Fig. 2 shows the ultraviolet-visible (UV-vis) absorption spectra of PBDFNTDO in chloroform solution and film states on quartz substrates, the absorption curve of PBDTNTDO-C3 film is also included for clear comparison. The corresponding results are listed in Table 1. The PBDFNTDO solution displays an absorption band in the wavelength range of 300–680 nm and the absorption peak is at 622 nm. The PBDFNTDO film shows an absorption band in the wavelength range of 300–750 nm and the absorption peak is at 627 nm. In the film state, the polymer shows red-shifted and broader absorption than that of the solution, the broader and better absorption originates from better planarity of the polymer and stronger electronic interaction between the individual polymer chains in the film states.[21] Compared to the PBDTNTDO-C3 film, the absorption peak of PBDFNTDO film has red-shifted *ca.* 70 nm, which indicates that this BDF based copolymer has stronger intermolecular interactions in the polymer chains or better chain stacking than that of the BDT based copolymer. The optical band gap (E_g) of the PBDFNTDO film calculated from the absorption band edge is *ca.* 1.65 eV. From the above analysis, PBDFNTDO is a lower bandgap polymer than PBDTNTDO-C3 (E_g^{opt}: 1.79 eV), which

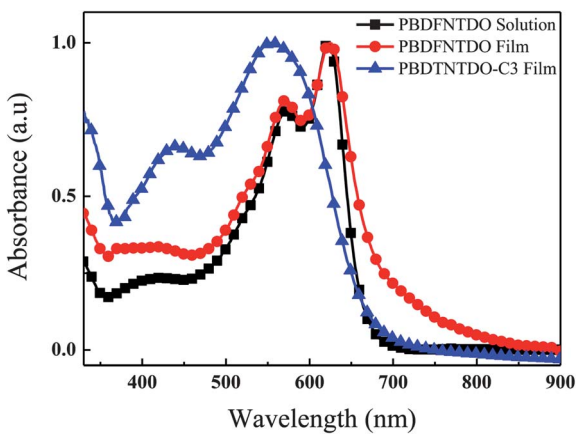

Fig. 2 UV-vis absorption spectra of PBDFNTDO in dilute $CHCl_3$ solution and PBDFNTDO, PBDTNTDO-C3 in the film states.

Table 1 Optical and electrochemical properties of PBDFNTDO and PBDTNTDO-C3

	Absorption spectra				Cyclic voltammetry		
	Solution	Film			p-doping	n-doping	
Polymers	λ_{max} (nm)	λ_{max} (nm)	λ_{onset} (nm)	E_g^{opt} (eV)	E_{on}^{ox}/HOMO (V)/(eV)	E_{on}^{red}/LUMO (V)/(eV)	E_g^{EC} (eV)
PBDFNTDO	622	627	750	1.65	0.63/−5.33	−1.3/−3.40	1.93
PBDTNTDO-C3	557	557	693	1.79	0.67/−5.27	−1.0/−3.53	1.67

may originate from the higher electronegativity of benzodifuran than benzodithiophene and stronger interactions in the polymer chains.

3.4 Electrochemical properties

The HOMO and LUMO levels of PBDFNTDO were measured by electrochemical cyclic voltammetry (CV). Fig. 3 shows the CV curve of PBDFNTDO film on a Pt electrode with 0.1 mol L^{-1} tetrabutylammonium hexafluorophosphate (Bu_4NPF_6)/acetonitrile (CH_3CN) as the electrolyte at a scan rate of 50 mV s^{-1}. The electrochemical data of PBDFNTDO are summarized in Table 1 and the corresponding data of PBDTNTDO-C3 are included for comparison. As shown in Fig. 3, it can be seen that PBDFNTDO exhibits quasi-reversible or reversible p-doping/dedoping (oxidation/re-reduction) processes over a positive potential range and quasi-reversible n-doping/dedoping (reduction/re-oxidation) processes over a negative potential range. We calculated the HOMO and LUMO energy levels of the polymer according to the equations:[13] HOMO = $-e(E_{on}^{ox} + 4.7)$ (eV); LUMO = $-e(E_{on}^{red} + 4.7)$ (eV). The onset reduction potential of PBDFNTDO is −1.3 V. The LUMO energy level of PBDFNTDO is −3.40 eV. The onset oxidation potential of PBDFNTDO is 0.63 V. The HOMO energy level of the polymer is −5.33 eV (see Fig. 4). The deep HOMO energy level of the PBDFNTDO is desirable for a high open circuit voltage of the PSCs based on the polymer donors. The electrochemical band-gap of 1.93 eV deduced from the electrochemical measurement is relatively higher than the optical bandgap due probably to the interface barrier for the charge injection from electrochemical measurement.

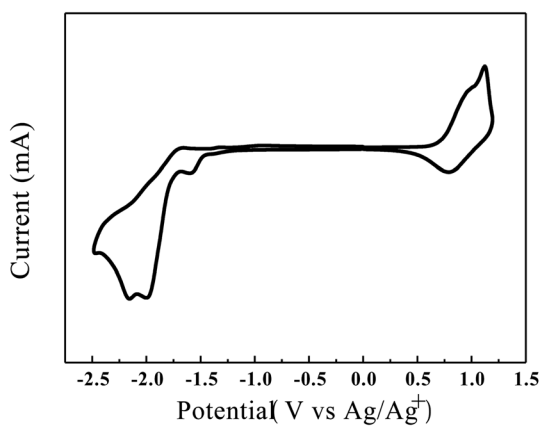

Fig. 3 Cyclic voltammogram of the PBDFNTDO film cast on a platinum disk in 0.1 mol L^{-1} Bu_4NPF_6/CH_3CN solution at 50 mV s^{-1}.

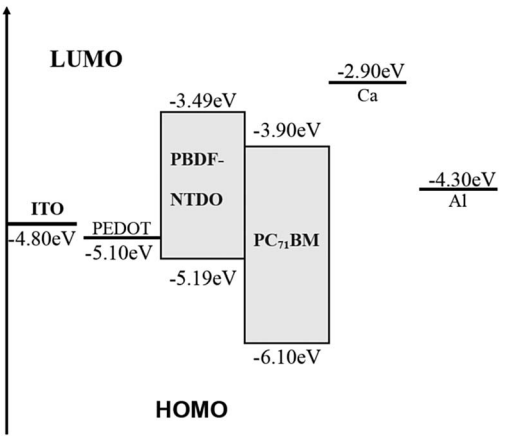

Fig. 4 Schematic energy level diagram of the PBDFNTDO based device.

3.5 Hole mobility

Besides the absorption and energy levels, hole mobility is another important factor for photovoltaic applications. We investigated the hole mobility of PBDFNTDO by SCLC method which is based on Poole–Frenkel Law[24] with a device structure of ITO/PEDOT:PSS/PBDFNTDO:$PC_{71}BM$ (1 : 1.5, w/w)/Au. SCLC is described by

$$J_{SCLC} = \frac{9}{8}\varepsilon_0\varepsilon_r\mu_0\frac{(V - V_{bi})^2}{d^3}\exp\left[0.89\gamma\sqrt{\frac{V - V_{bi}}{d}}\right] \quad (1)$$

The results are plotted as $\ln(Jd^3/V^2)$ *vs.* $(V/d)^{0.5}$, as shown in Fig. 5. Here, J stands for current density, d is the thickness of the device, and $V = V_{appl} - V_{bi}$, where V_{appl} is the applied potential and V_{bi} is the built-in potential. According to eqn (1),[13] the average hole mobility of the PBDFNTDO/$PC_{71}BM$ blend is 5.0×10^{-3} cm^2 V^{-1} s^{-1} over five devices. The hole mobility of the PBDFNTDO blend was much higher than that of the PBDTNTDO-C3 blend (3.0×10^{-5} cm^2 V^{-1} s^{-1}) and the PBDFDTBT blend (8.9×10^{-4} cm^2 V^{-1} s^{-1})[21] in the same conditions, presumably because of the larger planar structure and close stacking of PBDFNTDO, which is beneficial for obtaining a higher mobility. At the same time, we measured the hole mobility of the single polymer PBDFNTDO using SCLC method, interestingly PBDFNTDO exhibits very similar hole mobility compared with its blend with PCBM. To further verify this result, we measured the field effect transistors (FETs) of PBDFNTDO, however, the PBDFNTDO just showed a moderate FET hole mobility of 2.1×10^{-4} cm^2 V^{-1} s^{-1}

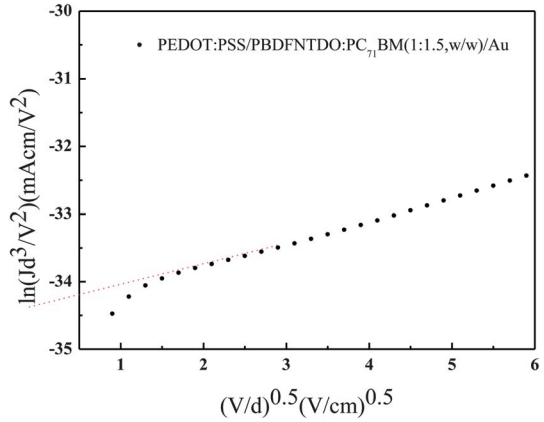

Fig. 5 $\ln(Jd^3/V^2)$ *vs.* $(V/d)^{0.5}$ plot of PBDFNTDO blend with $PC_{71}BM$ for measurement of the hole mobility by SCLC method.

(Fig. S1†). The FET mobility is not high, which might arise from the unoptimized device fabrications and the different mechanisms for PSCs and FETs.

3.6 X-ray analysis

To evaluate the crystallinity of PBDFNTDO and PBDTNTDO-C3, X-ray diffraction (XRD) measurements were taken from the spin-coated thick films on SiO_2 substrate. As shown in Fig. 6, the shapes of two copolymers are similar, no Bragg refraction peaks were observed for the two polymers, which show the copolymers are amorphous.

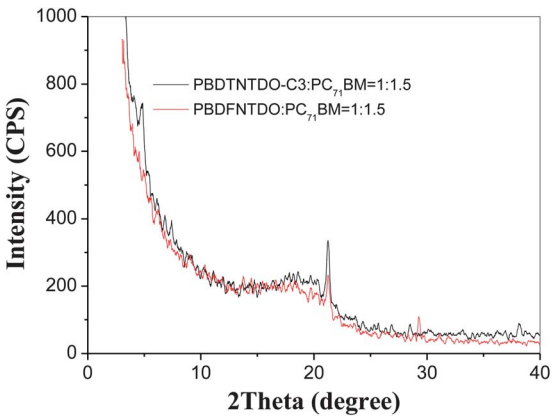

Fig. 6 XRD patterns of the PBDFNTDO and PBDTNTDO-C3 blends with PCBM thin films.

3.7 Photovoltaic properties

With its broad absorption and appropriate energy levels combined with high hole mobility, our newly synthesized polymer should lead to some high photovoltaic properties. The bulk heterojunction PSCs were fabricated with a device structure of ITO/PEDOT:PSS/PBDFNTDO:PCBM/Ca/Al to investigate the photovoltaic properties of PBDFNTDO. Fig. 7 shows the *J–V* curves of the devices under the illumination of AM 1.5 G, 100 mW cm^{-2} and the corresponding open-circuit voltage (V_{oc}), short circuit current (J_{sc}), fill factor (FF), and

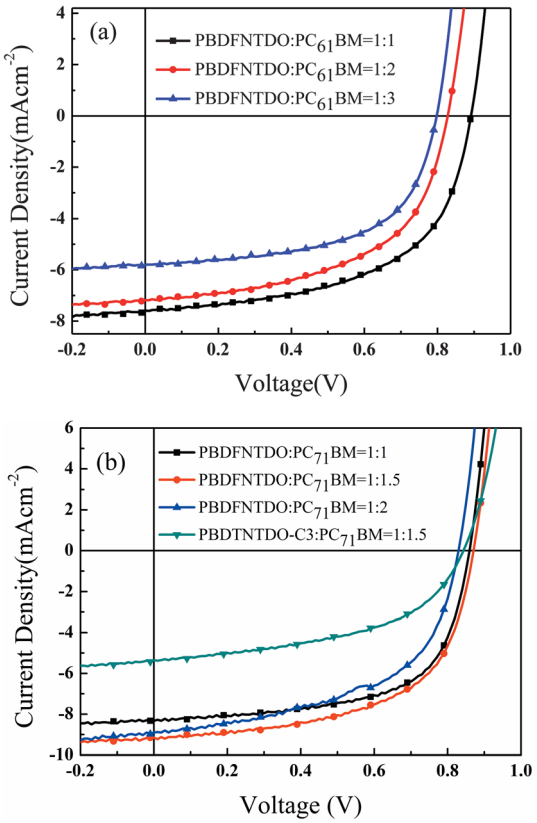

Fig. 7 *J–V* curves of the polymer solar cells based on (a) PBDFNTDO:$PC_{60}BM$ with different weight ratios; (b) PBDFNTDO:$PC_{71}BM$ with different weight ratios and PBDTNTDO-C3:$PC_{71}BM$ (1 : 1.5) in ODCB.

power conversion efficiency (PCE) are also summarized in Table 2. First, the different weight ratios of PBDFNTDO to PCBM were investigated to optimize the device performance. With blends of PBDFNTDO and $PC_{60}BM$ in weight ratios of 1 : 1, 1 : 2, 1 : 3, respectively, their *J–V* curves are shown in Fig. 7a. With PBDFNTDO and $PC_{60}BM$ in : 1 weight ratio, the best PCE of 3.84% was obtained with a V_{oc} of 0.96 V, J_{sc} of 7.6 mA cm^{-2} and FF of 0.56, respectively. With the content of $PC_{60}BM$ increasing, the PCE of the devices reduced significantly, which is due to $PC_{60}BM$ having a narrow absorption band, resulting in decreased J_{sc} of the devices. In order to obtain a better PCE of the PSCs, we replaced $PC_{60}BM$ with $PC_{71}BM$, because $PC_{71}BM$ has a better absorption than $PC_{60}BM$ while keeping a similar energy level, meaning that higher J_{sc} of the devices is expected. As shown in Fig. 7b, compared with $PC_{60}BM$ as acceptor, for PBDFNTDO and $PC_{71}BM$ in weight ratios of 1 : 1, 1 : 1.5, 1 : 2, in all cases PCEs of above 4.0% were obtained. The higher PCEs obtained are mainly from the increased J_{sc}, as expected. When the weight ratio of PBDFNTDO to $PC_{71}BM$ is 1 : 1.5, the best PCE of 4.71% with a V_{oc} of 0.87 V, a J_{sc} of 9.14 mA cm^{-2}, and a FF of 0.59 was achieved. Such a high V_{oc} of almost 0.9 V is consistent with the deep-lying HOMO energy level of PBDFNTDO. Compared with PBDTNTDO-C3 (the highest PCE = 2.27% for a weight ratio of 1 : 1.5 of PBDTNTDO-C3 to $PC_{71}BM$ blend in the same conditions), PBDFNTDO achieved a PCE

Table 2 Photovoltaic properties of PSCs based on PBDFNTDO:PCBM and PBDTNTDO-C3:$PC_{71}BM$ (1 : 1.5)

Active layer	V_{oc} (V)	J_{sc} (mA cm^{-2})	FF (%)	PCE (%)
PBDFNTDO:$PC_{60}BM$ = 1 : 1	0.89	7.58	57.0	3.84
PBDFNTDO:$PC_{60}BM$ = 1 : 2	0.83	7.17	54.8	3.26
PBDFNTDO:$PC_{60}BM$ = 1 : 3	0.80	5.79	58.9	2.73
PBDFNTDO:$PC_{71}BM$ = 1 : 1	0.86	8.32	62.6	4.48
PBDFNTDO:$PC_{71}BM$ = 1 : 1.5	0.87	9.14	59.2	4.71
PBDFNTDO:$PC_{71}BM$ = 1 : 2	0.83	8.90	54.1	4.00
PBDTNTDO-C3:$PC_{71}BM$ = 1 : 1.5	0.84	5.34	50.6	2.27

more than two-fold higher, because PBDFNTDO possessed better, broad absorption and especially higher hole mobility than BDTNTDO-C3 which led to a higher J_{sc} and FF. PCE of the devices with a D/A ratio of 1 : 1.5 is higher than that of the other ratios. The devices with 1 : 1.5 weight ratio of PBDFNTDO/$PC_{71}BM$ were further optimized by using 1,8-diiodooctane (DIO) (0.5%, v/v) as the processing additive and thermal annealing (90 °C, 10 min) according to reported work.[25] Unregretfully, the results show DIO and thermal annealing do not make big changes to the device properties, even PCEs are lowered because of slightly lower J_{sc} and FF with a slightly higher V_{oc} of up to 0.93 V as shown in Fig. S2 and Table S1†. Further device modifications are in progress, we firmly believe PCEs can be improved after careful device optimization. To clarify the high photovoltaic properties of PBDFNTDO based devices, we did external quantum efficiency (EQE) measurements. Fig. 8 shows EQE plots of the PSC devices under the illumination of monochromatic light. In both graphs, the shapes of the EQE plots are similar to the absorption spectra of the films, indicating that all the absorption wavelengths of PBDFNTDO contributed to photocurrent generation. The EQE of the blend from PBDFNTDO and $PC_{71}BM$ is higher for the absorption wavelengths especially from 300–400 nm, which originates from the better absorption from $PC_{71}BM$ than $PC_{60}BM$. The higher value of EQE is consistent with the higher J_{sc} measured in the PSCs.

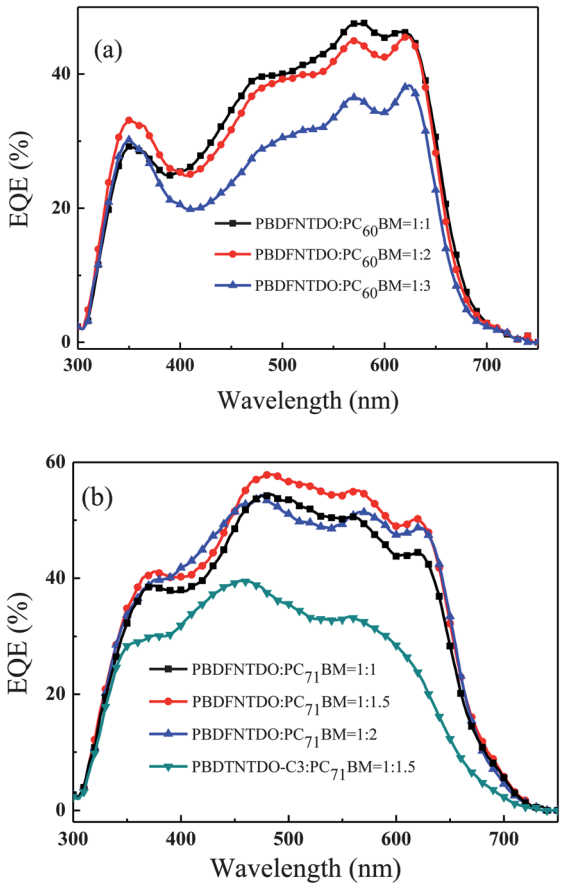

Fig. 8 The EQE values of the PSCs based on (a) PBDFNTDO:$PC_{60}BM$ with different weight ratios; (b) PBDFNTDO:$PC_{71}BM$ with different weight ratios and PBDTNTDO-C3:$PC_{71}BM$ (1 : 1.5) in ODCB for comparison.

3.8 Morphology

Besides absorption, energy level and mobility, the morphology of the photoactive layer is very important for PSCs, and in some cases the performance of the device strongly depends on its morphological characteristics. Therefore, we investigated the morphologies of PBDFNTDO and $PC_{71}BM$ blends spin-coated from their *o*-dichlorobenzene (ODCB) solutions using tapping-mode atomic-force microscopy (AFM). Fig. 9 shows the height and phase images of PBDFNTDO:$PC_{71}BM$ (1 : 1.5, w/w) films. From the height image, rough surfaces with relatively large aggregates were observed, which may be compact chain packing and aggregate crystallization, beneficial for obtaining high hole mobility. As shown in the corresponding phase image, pronounced nanophase separation was formed, which to some extent explains the high photovoltaic properties of the PBDFNTDO/PCBM blend.[26]

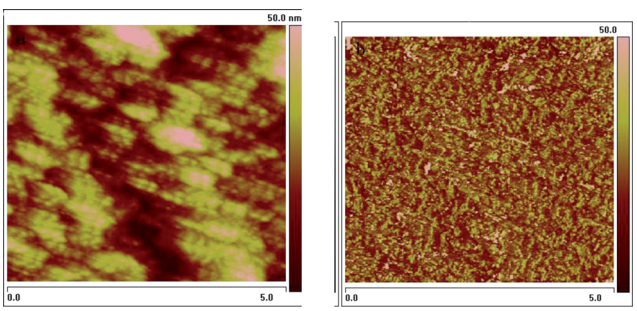

Fig. 9 AFM images (5 μm × 5 μm) of PBDFNTDO:$PC_{71}BM$ (1 : 1.5, w/w) in ODCB: (a) height image; (b) phase image.

4. Conclusions

In summary, a new benzo[1,2-*b*:4,5-*b*′]difuran containing donor–acceptor polymer (PBDFNTDO) has been synthesized and applied in PSCs. The polymer possesses good thermal stability, broad absorption and low-lying HOMO energy levels. The hole mobility of the blend reached up to 5.0×10^{-3} cm^2 V^{-1} s^{-1}. A PCE of 4.71% from a PBDFNTDO based polymer solar cell with $V_{oc} = 0.87$ V, $J_{sc} = 9.14$ mA cm^{-2}, and FF = 59% was obtained, and higher photovoltaic performance will be highly anticipated after combining elaborate device fabrications with rational material designs. Compared to its similar polymer PBDTNTDO-C3, PBDFNTDO exhibited much better properties, which indicates that PBDFNTDO is a promising candidate for high-efficiency polymer solar cells and the benzodifuran unit probably is an excellent electron donating building block for photovoltaic polymeric materials.

Acknowledgements

In this work, Dr Bo Liu did the organic synthesis and Xuewen Chen performed the characterizations. We also thank Dr Xinjun Xu and Prof. Lidong Li from University of Science and Technology Beijing for FET measurements. This work was supported by NSFC (nos. 51173206, 21161160443), National High Technology Research and Development Program (no. 2011AA050523), the Natural Science Foundation of Hunan Province, China (no. 11JJ4010), China Postdoctoral Science Foundation (no. 20110490150) and the Fundamental Research Funds for the Central Universities (no. 2010QZZD0112).

References

1 Y. Cheng, S. Yang and C. Hsu, *Chem. Rev.*, 2009, **11**, 5868.
2 T. Lei, Y. Cao, Y. Fan, C. Liu, S. Yuan and J. Pei, *J. Am. Chem. Soc.*, 2011, **133**, 6099.
3 H. Wu, L. Ying, W. Yang and Y. Cao, *Chem. Soc. Rev.*, 2009, **38**, 3391.
4 S. Park, B. Roy, C. Coates, J. Moon, D. Moses, M. Leclerc, K. Lee and A. Heeger, *Nat. Photonics*, 2009, **3**, 297.
5 Y. Li and Y. Zou, *Adv. Mater.*, 2008, **20**, 2952.
6 B. Liu, W. Wu, B. Peng, Y. Liu, Y. He, C. Pan and Y. Zou, *Polym. Chem.*, 2010, **1**, 678.
7 J. Chen and Y. Cao, *Acc. Chem. Res.*, 2009, **42**, 1709.
8 E. Zhou, S. Yamakawa, K. Tajima, C. Yang and K. Hashimoto, *Chem. Mater.*, 2009, **21**, 4055.
9 G. Yu, J. Gao, J. Hummelen, F. Wudl and A. J. Heeger, *Science*, 1995, **270**, 1789.
10 Z. Zhang, B. Peng, B. Liu, C. Pan, Y. Li, Y. He, K. Zhou and Y. Zou, *Polym. Chem.*, 2010, **1**, 1441.
11 Y. Zou, D. Gendron, R. Neagu-Plesu and M. Leclerc, *Macromolecules*, 2009, **42**, 6361.
12 T. Johansson, W. Mammo, M. Svensson, M. Andersson and O. Inganas, *J. Mater. Chem.*, 2003, **13**, 1316.
13 Z. Zhang, J. Min, S. Zhang, J. Zhang, M. Zhang and Y. Li, *Chem. Commun.*, 2011, **47**, 9474.
14 Z. He, C. Zhong, X. Huang, W. Wong, H. Wu, L. Chen, S. Su and Y. Cao, *Adv. Mater.*, 2011, **23**, 4626.
15 J. Hou, M. Park, S. Zhang, Y. Yao, L. Chen, J. Li and Y. Yang, *Macromolecules*, 2008, **41**, 6012.
16 Y. Zou, A. Najari, P. Berrouard, S. Beaupré, R. Aich, Y. Tao and M. Leclerc, *J. Am. Chem. Soc.*, 2010, **132**, 5330.
17 Y. Liang, Y. Wu, D. Feng, S. Tsai, H. Son, G. Li and L. Yu, *J. Am. Chem. Soc.*, 2009, **1**, 56.
18 Y. Zou, D. Gendron, R. Neagu-Plesu and M. Leclerc, *Macromolecules*, 2009, **42**, 6361.
19 H. Chen, J. Hou, S. Zhang, Y. Liang, G. Yang, Y. Yang, L. Yu, Y. Wu and G. Li, *Nat. Photonics*, 2009, **3**, 649.
20 C. Cui, X. Fan, M. Zhang, J. Zhang, J. Min and Y. Li, *Chem. Commun.*, 2011, **47**, 11345.
21 L. Huo, Y. Huang, B. Fan, X. Guo, Y. Jing, M. Zhang, Y. Li and J. Hou, *Chem. Commun.*, 2012, **48**, 3318.
22 J. Hou, H. Chen, S. Zhang and Y. Yang, *J. Phys. Chem. C*, 2009, **113**, 21202.
23 X. Chen, B. Liu, Y. Zou, W. Tang, Y. Li and D. Xiao, *RSC Adv.*, 2012, DOI: 10.1039/c2ra20747h.
24 W. Pasveer, J. Cottaar, C. Tanase, R. Coehoorn, P. Bobbert, P. Blom, D. Leeuw and M. Michels, *Phys. Rev. Lett.*, 2005, **94**, 206601.
25 W. Ma, C. Yang, X. Gong, K. Lee and A. Heeger, *Adv. Funct. Mater.*, 2005, **15**, 1617.
26 W. Li, Y. Zhou, B. V. Andersson, L. M. Andersson, Y. Thomann, C. Veit, K. Tvingstedt, R. Qin, Z. Bo, O. Inganas, U. Würfel and F. Zhang, *Org. Electron.*, 2011, **12**, 1544.